IOP Conf. Series: Materials Science and Engineering **739** (2020) 012037 doi:10.1088/1757-899X/739/1/012037

Thermal Simulation and Sonoporation Experiment Based on a Focused Ultrasonic System

Zihong Liu[1, 2, 3], Hui You[1,3*], Ping Zhang[1], Ronghui Lin[1], Yongjia Chang[3]

[1]Department of Precision Instrumentation and Machinery, University of Science and Technology of China, Hefei 230026, Anhui, China
[2]Key Laboratory of Testing Technology for Manufacturing Process of Ministry of Education, Southwest University of Science and Technology, Mianyang 621010, Sichuan, China
[3]Institute of Intelligent Machines, Chinese Academy of Science, Hefei230031, Anhui, China

usmlhy@iim.ac.cn

Abstract. This paper aims at analyzing ultrasonic thermal effect and sonoporation based on a focused ultrasonic experiment system. The numerical analysis, about cavitaion conditions and ultrasonic thermal effect using the coupling model of pressure acoustic and bioheat transfer, were given, in which the temperature rise trend is identical to the conclusion in the literature [2]. According to the simulation analysis of ultrasonic thermal effect, temperature rise is approximately 18.5K near the focal spot with Ultrasonic radiation for 60s, which had little effect on 293T cell viability. In the acoustic chemical experiment, 293T cell viability is about 85% at 60s of the ultrasound irradiation, which was observed by 200× fluorescence microscope. The cell states of survival and abnormal was observed and analyzed in the sonoporation experiment at 60s of ultrasonic time.

1. Introduction

When the ultrasound passes through a volume of cell solution, some of the primary energy is absorbed locally by the solution and turned into heat, which results in a temperature increase [1-5]. In terms of the focused ultrasound and ultrasonic thermal effect, focused ultrasound has been applied in ultrasound hyperthermia [6, 7] and focused ultrasound surgery [8, 9], and theory study on temperature rise has been given [1, 2]. However, the numerical analysis of ultrasonic thermal effect and cavitation in cell solution has not been elucidated, and there have been few studies on sonoporation experiment involving ultrasonic thermal effect.

To elucidate ultrasonic thermal effect and sonoporation in cell solution under high frequency ultrasonic transducer, a focused ultrasonic experiment system was set up [10]. Based on the ultrasonic cavitation conditions deduced by Blake threshold pressure and the Keller-Miksis equation [11], the ultrasonic parameters in coupling simulation model was determined, and the numerical analysis of

ultrasonic thermal effect was given based on homogeneous Helmholtz equation [12] and Pennes' Bioheat Transfer equation [13].

In the experiment, sonoporation experiment with ultrasonic thermal effect was carried out by acoustic chemistry testing [14, 15]. Cell perforation and cell viability were tested respectively using PI and FDA, which was observed by fluorescence microscope.

2. Experimental setups and methods

2.1. Experimental model

Figure 1 shows sonoporation experimental system with ultrasonic induced heating based on a focused ultrasonic transducer. In this experimental system, the cell solution in the beaker was put in the focused sound field, and the geometric center of the cell solution was almost at the focus of the transducer. In this study, when the focused ultrasound from the ultrasonic transducer passed though the cell solution, some of the energy was absorbed locally by the solution and turned into the heat or facilitated cavitation which was used to transitorily increase sonoporation in cell membrane permeability [16, 17]. In order to reduce the heating effect of the transducer components, the convection channel was designed as shown in figure 1.

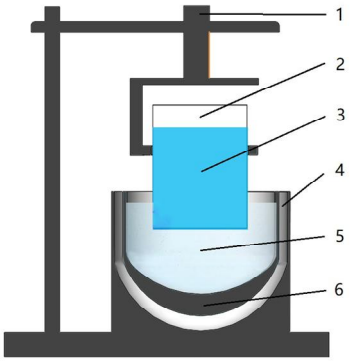

1.Screw micrometer. 2.Beaker. 3.The cell solution.
4.Convection channel. 5.Water. 6.Focused ultrasonic transducer.

Figure 1. Experimental setup used for sonoporation with ultrasonic induced heating.

2.2. Mechanistical modeling base

According to the van der Waals equation [18], the pressure in or out the micro bubble is equal when the bubble is in equilibrium.

$$P_g\left(\frac{R_0}{R}\right)^3 = P_h - P_V + \frac{2\sigma}{R} \tag{1}$$

Where, P_V is the vapour pressure in the bubble, $P_g\left(=P_h+2\sigma/R_0\right)$ is the gas pressure in the bubble, P_h is the fluid pressure, and σ is the coefficient of surface tension.

To obtained minimum pressure out the bubble when bubble radius changes, the critical radius could be solved by taking the derivative of R in equation (1). And Blake threshold pressure P_B could be gained from the critical radius and equation (1):

$$P_B = P_h + \frac{2}{3}\left[\frac{\left(\frac{2\sigma}{R_0}\right)^3}{3(P_h + \frac{2\sigma}{R_0})}\right]^{\frac{1}{2}} \tag{2}$$

In the study, the radial dynamics of the micro bubble was described by the Keller-Miksis equation [11]:

$$\rho\left[R\frac{d^2R}{dt^2} + \frac{3}{2}\left(\frac{dR}{dt}\right)^2\right] = \left[P_g - P_h - P(t)\right] - \frac{4\mu}{\rho R}\frac{dR}{dt} - \frac{2\sigma}{R} \tag{3}$$

In this equation, ρ and μ denote the fluid density and shear viscosity of the fluid. Here, driving pressure $P(t)$ applied on bubbles can be approximated by acoustic pressure $P_{\mathrm{a}}\ (=-P_{\mathrm{A}}\sin(\omega t))$. P_{A} refers to the acoustic pressure amplitude and $f(=\frac{\omega}{2\pi})$ refers to the acoustic pressure frequency.

By ignoring the shear viscosity of the fluid, the equation (3) is expended to the $1/R_0$ power when bubble radial is $R\ (=R_0+r,\ \ r<R)$:

$$r^2 + \omega_r{}^2 r = \frac{P_A}{\rho R_0}\sin\omega_a t \tag{4}$$

According to equation (4), the resonance frequency $f_r\left(=\frac{\omega_r}{2\pi}\right)$ of the bubble was given by Minneart. And bubble vibration is obvious when the ultrasonic frequency(f_a) is equal to f_r

$$f_r = \frac{1}{2\pi R_0}\left[\frac{3}{\rho}\left(P_h + \frac{2\sigma}{R_0}\right)\right]^{\frac{1}{2}} \tag{5}$$

According to equation (2) and equation (4), microbubble cavitation could occur when $P_A > P_B$ and $f_a < f_r$.

2.3. Computational model and boundary conditions

2.3.1. Acoustics and thermodynamics coupling based on the system. It is assumed that the acoustic wave propagation is linear. Nonlinear effects and shear waves are neglected. In 2D axisymmetric cylindrical coordinates, the wave equation of the ultrasonic pressure is solved by the homogeneous Helmholtz equation:

$$\frac{\partial}{\partial r}\left[\frac{r}{\rho_c}\left(\frac{\partial p}{\partial r}\right)\right] + r\frac{\partial}{\partial z}\left[\frac{1}{\rho_c}\left(\frac{\partial p}{\partial z}\right)\right] - \left[\left(\frac{\omega}{c_c}\right)^2\right]\frac{rp}{\rho_c} = 0 \tag{6}$$

In this equation, the density ρ_c and the speed of sound c_c are complex-valued to account for the material's damping properties. In the acoustic field obtained by equation (6), the heat source $\mathrm{Q}\left(=2\alpha I\right)$ for thermal simulation could be by gained by the following equation:

$$Q = 2\alpha \left| \mathrm{Re}\left(\frac{1}{2} p\upsilon \right) \right| \tag{7}$$

In this equation, the ultrasonic parameters α , I , p and υ denote the ultrasonic absorption coefficient, ultrasonic intensity magnitude, ultrasonic pressure and the ultrasonic particle velocity vector, respectively. By taking ultrasonic heat source Q into the Pennes' Bioheat Transfer equation, the temperature of the cell solution could be obtained.

$$\rho c_p \frac{\partial T}{\partial t} = \nabla \cdot (k \nabla T) - \rho c_p \omega_p (T - T_0) + Q + Q_m \tag{8}$$

Where, ρ , c_p and k respectively denote the density, the specific heat and the thermal conductivity, . And ω_p , Q and Q_m respectively refer to the solution perfusion rate (here, $\omega_p = 0$), the heat source obtained by equation (7) and the biologic heat source.

2.3.2. Simulation model and Boundary conditions. Figure 2 shows the geometry of the ultrasonic transducer and cell solution phantom in the simulation model. Both the cell solution in the utensil and the bowl-shaped transducer are immersed in water. Four cylindrical perfectly matched layers(PMLs) (1-3 and 7 in figure 2) are used to absorb the outgoing ultrasonic waves. In the simulation model, the normal displacement of the transducer was set to 3.8nm according to the transducer characteristics (WHQ2018).

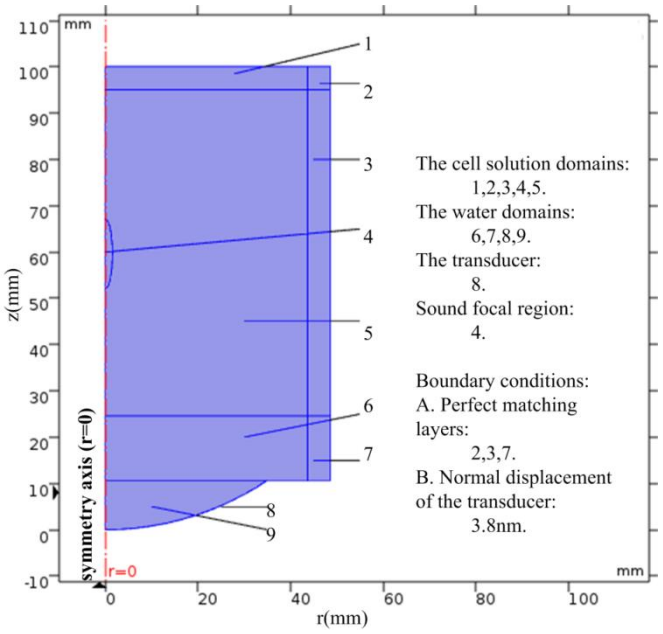

Figure 2. Geometric and physical model for numerical simulation.

The software COMSOL Multiphysics (Version 5.3) was used to carried out the grid division and numerical simulation. Based on the finite difference method(FDM) [19], pressure acoustics (acpr) and bioheat transfer (ht) were employed, which the pressure acoustics simulation is performed in all domains and the heat transfer model is only applied in the cell solution domain. Through the grid

division, 703221 DOF was obtained in acoustic pressure model and 8126 DOF was obtained in bioheat transfer model.

2.4. Test methods of sonoporation experiment

Due to thermal effect of the ultrasound, the temperature rises with ultrasonic action time, which determines the characteristics of cell perforation and cell activity. With suitable cell solution temperature determined by numerical analysis, cell membrane perforation and cell activity could be separately test using propidium iodide (PI) and fluorescein diacetate(FDA). According to the sonoporation, the permeability of cell membranes is improved under ultrasound, which permits the macromolecules and DNA fragments near the cell to penetrate the cell membrane into the cell [20, 21]. However, the cell membrane would be deadly damaged when exposed to ultrasound, which is beyond repair. To conform the reates of cell membrane perforation and cell activity, four tested solutions were employed with 200× fluorescence microscope (Lecia DMI4000B, Germany):

(i). The cell solution (2.0×106/ml), cultured using human embryonic kidney cells(293T), is used to quantify the ultrasonic thermal effect in the experimental platform.

(ii). The 293T cell solution (2.0×106/ml) with PI is used to test cell membrane perforation. The testing mechanism is that the PI permeates only through damaged cell membranes and produces red fluorescence.

(iii). The 293T cell solution (2.0×106/ml) with FDA is used to test cell activity. The testing mechanism is that FDA permeates only through living cell membranes and produces green fluorescence when the cell is living.

(iv). The 293T cell solution (2.0×106/ml) with PI and FDA is used for comparative testing.

In our experiment, the rates of cell membrane damaged, cell viability and cell transfection were tested respectively by above solution with the same condition.

3. Results and discussion

3.1. Numerical simulation

According to equation (7) and equation (3), the resonance frequency of the bubble is $f_r\,(=1.34MHz)$ with the initial bubble radius R_0 (=3.6 μm) when $P_h\,(=1.013\times10^5 P_a)$ and $\sigma\,(=0.076Nm^{-1})$ are determined, and Blake threshold pressure is $P_B\,(=1.159\times10^5 P_a)$ which is greater than actual value in the experiment system. The transducer, drive frequency 1.045MHz and ultrasonic power 3.78w, is employed in the experiment.

Figure 3 shows acoustic pressure distribution in the cell solution in numerical simulation. According to ultrasonic cavitation conditions deriveed above, the cavitation comes into being in some regions where the acoustic pressure P_A is greater than P_B with $f_a < f_r$ (as figure 3.(a) shown), especially in and near the sound focal area as figure 3.(b) and figure 3.(c) shown.

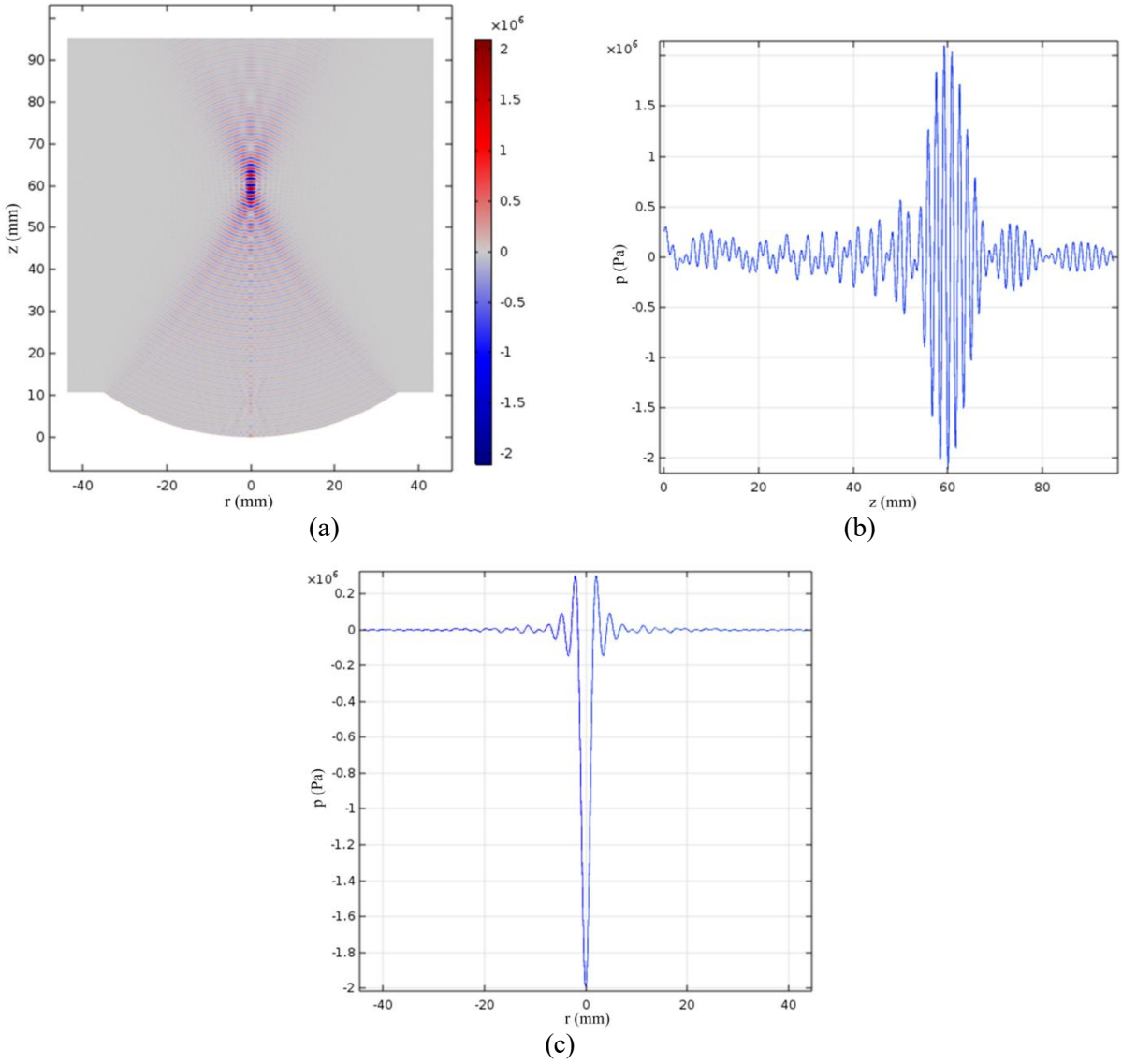

(a). Acoustic pressure in cell solution. (b). Acoustic pressure on z axial.
(c). Acoustic pressure on radius direction at sound focal spot

Figure 3. acoustic pressure distribution in cell solution (fa=1.045MHz).

In numerical simulation about ultrasonic thermal effect in cell solution, the values of the physical constants used are given in Table 1 [1, 2].

Table 1. Values of physical properties.

Name	Property	Value	Unit
ρ	Density	1044	Kg/m^3
c_p	Heat capacity at constant pressure	3370	$J/(kg \cdot K)$
k	Thermal conductivity	0.45	$W/(m \cdot K)$
T0	Room temperature	273	K
α	Ultrasonic absorption coefficient	8	1/m

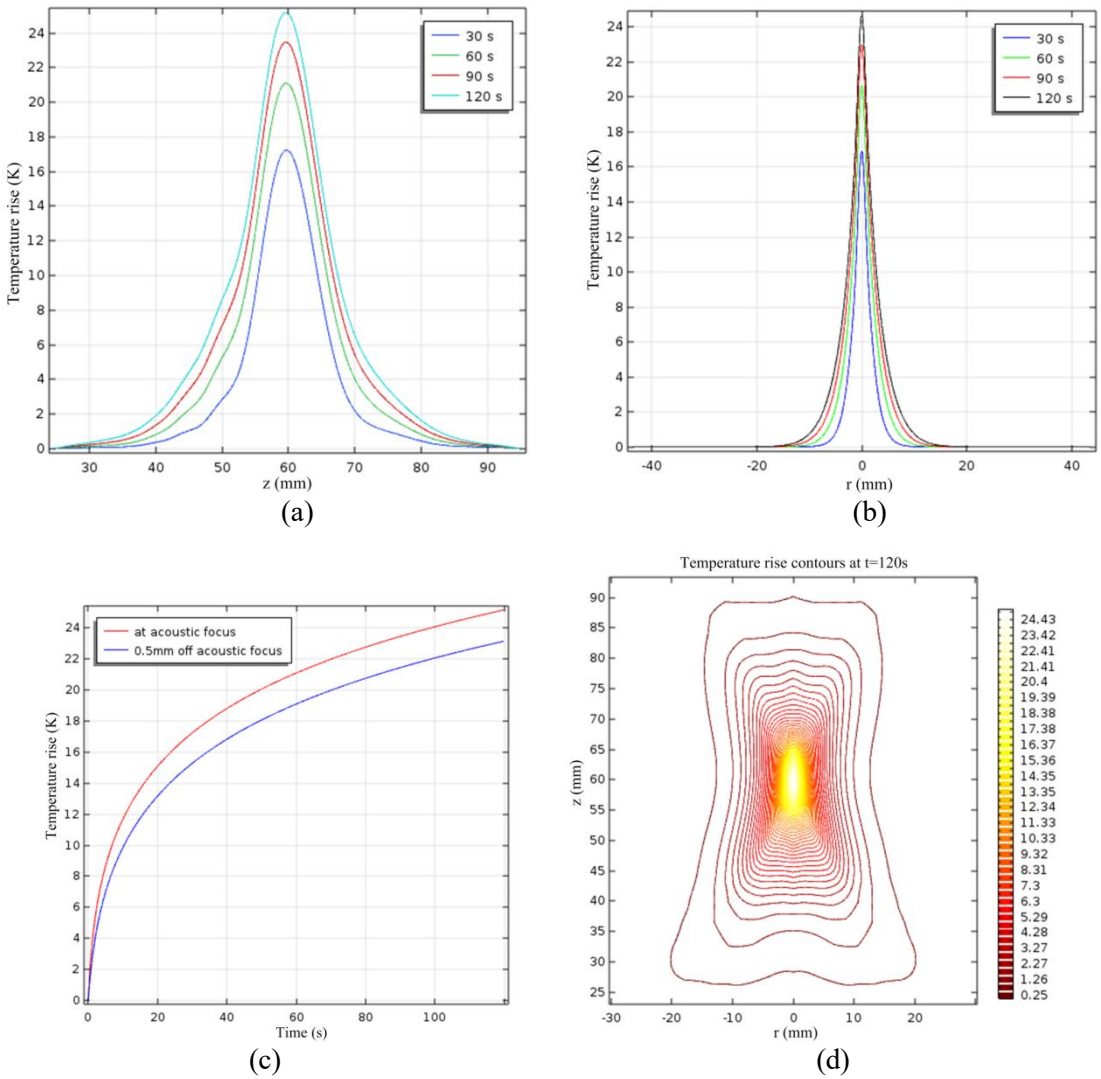

(a). Temperature rise on z axial. (b). Temperature rise on radius direction at sound focal spot. (c). Temperature rise at and 0.5 ㎜ off acoustic focus. (d). Temperature rise contours at 120 sec.

Figure 4. Temperature rise under ultrasonic irradiation in cell solution.

Figure 4 shows temperature rise under ultrasonic irradiation in cell solution. According to the simulation results shown in figure 4. (a) and figure 4. (b), ultrasonic focused spot is the high-temperature area and the fastest temperature rise area, which is an ellipse region with axial length of 15mm and 3mm. Figure.4. (c) shows temperature rise at acoustic focus and 0.5mm off acoustic focus, which indicates that temperature rise trend in the figure is identical to the conclusion in the literature (See figure 3 in the literature [2]). As the temperature difference increases in the cell solution, temperature rises slowly after 20s (As shown in figure 4. (c)). In the numerical simulation of ultrasonic thermal effect, the temperature is 24.43K hotter than room temperature T0(273K) when ultrasonic action time is 120s in and near the ultrasonic focal spot area. Figure 4. (d) shows temperature rise contours at 120s, in which the high-temperature area is at ultrasonic focused ellipse region.

3.2. Sonoporation experiment

Figure 5 shows 293T cell viability under ultrasonic in the acoustic chemistry experiment. Due to ultrasonic thermal effect and ultrasonic cavitation in the cell solution, cell viability declines rapidly after 60s of ultrasonic irradiation. In the acoustic chemistry experiment, cell viability is about 85% at 60s, which is meaningful for study on sonoporation.

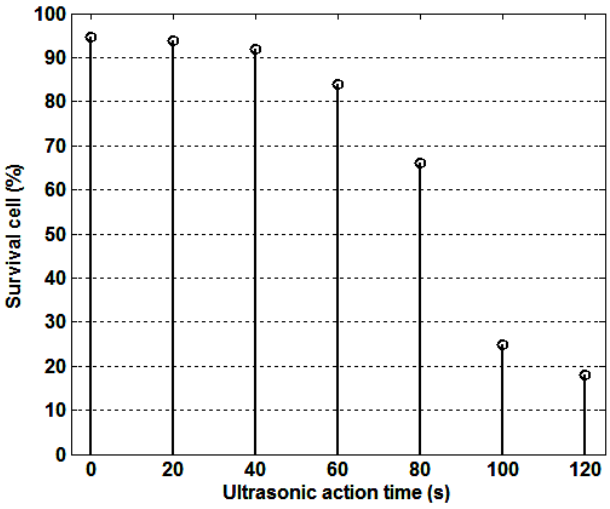

Figure 5. Cell viability with ultrasound action time.

The experimental temperature of 293T cell solution should be similar to human body temperature for the sonoporation experiment, that ultrasonic action time was set to no more than 60s in sonoporation experiments according to ultrasonic thermal simulation.

Figure 6 shows the images of cell marked with FDA fluorescence or PI fluorescence, which is obtained by experimental treatment at 60s of ultrasonic radiation [22]. In the acoustic chemistry experiment, the cavitation and sonoporation come into being, which could be testified by cell membrane damage shown in figure 6. 293T cells with green fluorescence indicate that the cells are living, which contain cells of membranes perforated and cells of repaired membranes. 293T cells with red fluorescence indicate that the cell membrane is damaged by bubble cavitation, which is dead or will repair the cell membranes itself.

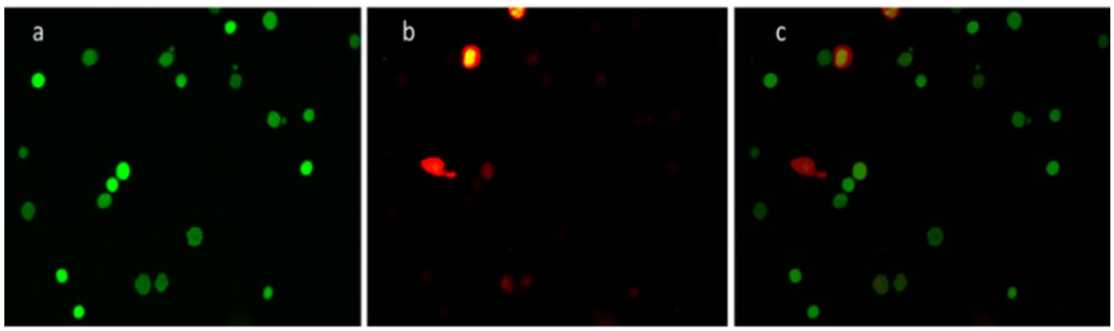

(a). Living cell with FDA fluorescence. (b). Damaged cell with PI fluorescence.
(c). Cell with fluorescence form FDA and PI.

Figure 6. Acoustic chemistry experiment on 293T (PI and FDA) (with a 200× lens).

4. Conclusion

This study shows that thermal effect of ultrasound in cell solution is obvious and cell membrane permeability is increased in the focused ultrasonic experimental system.

According to the result of numerical analysis, cavitation comes out under ultrasound ($f_a = 1.04MHz$) and temperature rise is efficient, which is highly consistent with ultrasonic thermal simulation. The temperature rise is about 18.5K when 293T cell solution is under ultrasound 60 seconds according to ultrasonic thermal simulation, which is benefit for cell to live and sonoporation experiment. In line with the acoustic chemistry experiments, the percentage of cell viability is approach to 85% with ultrasonic radiation for 60s.

Acknowledgements

The authors are grateful for the support provided by National Natural Science Foundation of China (Grant No.61176105), and Sichuan Education Department Program, China (Grant No.14ZB0112).

References

[1] Parker K J 1983 The thermal pulse decay technique for measuring ultrasonic absorption coefficients, *J. Acoustic. Soc. America* **74(5)** 1356-61.
[2] Clarke R L, Ter Haar G R 1997 Temperature rise recorded during lesion formation by high-intensity focused ultrasound, *Ultrasound Medic Bio*. **23(2)** 299-306.
[3] Ter Haar G 2007 Therapeutic applications of ultrasound, *Prog. Biophys. Molec. Bio*. **93(1-3)** 111-29.
[4] Webb H, Lubner M G, Hinshaw J L 2011 Thermal ablation, *Semin. Roentgenol.* **46(2)** 133-41.
[5] Ahmed M, Brace C L, Lee Jr F T, Goldberg S N 2011 Principles of and advances in percutaneous ablation, *Radiology* **258(2)** 351-69.
[6] Hynynen K, Edwards D K 1989 Temperature measurements during ultrasound hyperthermia, *Medi. Physi*. **16(4)** 618-26.
[7] Seip R, Vanbaren P, Ebbini E S 1994 Dynamic focusing in ultrasound hyperthermia treatments using implantable hydrophone arrays, *IEEE Transa. Ultrason. Ferroelect. Freq. Contr*. **41(5)** 706-13.
[8] Tempany C M, Stewart E A, Mcdannold N, Quade B J, Jolesz F A, Hynynen K 2003 MR imaging–guided focused ultrasound surgery of uterine leiomyomas: a feasibility study, *Radiology* **226(3)** 897-905.
[9] Funaki K, Fukunishi H, Takayama T 2012 M481 symptom improvement after magnetic resonance-guided focused ultrasound surgery for uterine myomas, *Int. J. Gynecol. Obstetr*. **119** S685.
[10] Wang X, Gao J, Zhang P, Lin R, Yang Y, You H, Wang X 2015 Ultra-high frequency sonochemistry and its dosimetry, *Int. Conf. Info. Sci, Mach. Mater. Energ*. 1851-5.
[11] Mason T J, Lorimer J P, Bates D M, Zhao Y 1994 Dosimetry in sonochemistry: the use of aqueous terephthlate ion as a fluorescence monitor, *Ultraso. Sonochem*. **1(2)** S91-5.
[12] Moiola A, Hiptmair R, Perugia I 2011 Plane wave approximation of homogeneous Helmholtz solutions, *Journal of Applied Methematics and Physics*. **62(5)** 809-37.
[13] Ezzat M A, Alsowayan N S, Al-Muhiameed Z I, Ezzat S M 2014 Fractional modelling of pennes' bioheat transfer equation, *Heat Mass Transfer* **50(7)** 907-14.
[14] Blake J R, Taib B B, Doherty G 1986 Transient cavities near boundaries part 1 rigid boundary, *J. Fluid Mech*. **170** 479-97.
[15] Kudo N, Okada K, Yamamoto K 2009 Sonoporation by Single-Shot Pulsed Ultrasound with Microbubbles Adjacent to Cells, *Biophysic. J*. **96(12)** 4866-76.
[16] Stevenson D J, Gunnmoore F J, Campbell P, et al. 2010 Single cell optical transfection, *J. Roya. Soc. Interf*. **7(47)** 863-71.
[17] Heiser W C 2004 Delivery of DNA to cells in culture using particle bombardment, *Gene Deliv.*

Mannal. Cells. Human Press **245** 175-84.
[18] Lofstedt R, Weninger K, Putterman S, Barber B P 1995 Sonoluminescing bubbles and mass diffusion. *Phys. Rev. E* **51(5)** 4400.
[19] Sajjadi B, Raman A A A, Ibrahim S, Shah R S S R E 2012 Review on gas-liquid mixing analysis in multiscale stirred vessel using CFD, *Rev. Chem. Eng*. **28(2-3)** 171-89.
[20] Miller D L, Pislaru S V, Greenleaf J F 2002 Sonoporation: mechanical DNA delivery by ultrasonic cavitation, *Somatic Cell Molec. Geneti*. **27(1-6)** 115-34.
[21] Deng C X, et al. 2004 Ultrasound-induced cell membrane porosity, *Ultras. Medic. Bio*. **30(4)** 519-26.
[22] Zhang P 2016 Research on Gene Transfection by Ultrasound Method under the Microfluidic Environment, *Uni. Sci. Technol., China.*